

**Effects of temperature, acyl chain length, and flow-rate ratio on liposome formation and size in a microfluidic hydrodynamic focusing device**

Justin M. Zook and Wyatt N. Vreeland

**Abstract**

Microfluidic hydrodynamic focusing of an alcohol/lipid mixture into a narrow fluid stream by two oblique buffer streams provides a controlled and reproducible method of forming phospholipid bilayer vesicles (i.e., liposomes) with relatively monodisperse and specific size ranges. Previous work has established that liposome size can be controlled by changing the relative and absolute flow rates of the fluids. In other previous work, a kinetic (non-equilibrium) theoretical description of the detergent dilution liposome formation method was developed, in which planar lipid bilayer discs aggregate until they become sufficiently large to close into spherical liposomes. In this work, we show that an approximation of the kinetic theory can help explain liposome formation for our microfluidic method. This approximation predicts that the liposome radius should be approximately proportional to the ratio of the membrane bending elasticity modulus to the line tension of the hydrophobic edges of the lipid bilayer disc. In combination with very fast microfluidic mixing, this theory enables a new method to measure the ratio of the elasticity modulus to the line tension of membranes. The theory predicts that the temperature should change the liposome size primarily as a result of its effect on the ratio of the membrane bending elasticity modulus to the line tension, in contrast to previous work on microdroplet and microbubble formation, which showed that the effect of temperature on droplet/bubble size was primarily due to viscosity changes. In agreement with theory, most membrane compositions form larger liposomes close to or below the gel to liquid crystalline phase transition temperature, where the membrane elasticity modulus is much larger, and they have a much smaller dependence of size on temperature far above the transition temperature, where the membrane elasticity modulus is relatively

constant. Other parameters modulated by the temperature (e.g., viscosity, free energy, and diffusion coefficients) appear to have little or no effect on liposome size, because they have counteracting effects on the lipid aggregation rate and the liposome closure time. Experiments are performed using phospholipids with varying hydrophobic acyl chain lengths that have phase transition temperatures ranging from -1 °C to 55 °C, so that the temperature dependence is examined below, above, and around the transition temperature. In addition, the effect of IPA stabilizing the edges of the bilayer discs can be examined by comparing the liposome sizes obtained at different flow rate ratios. Finally, polydispersity is shown to increase as the median liposome size increases, regardless of whether the change in size is due to changing temperature or flow rate ratio.

Keywords: liposome formation theory, phase transition temperature, microfluidic vesicle formation, planar bilayer fragment model, cholesterol

## **Introduction**

Liposomes are spherical vesicles made of phospholipid bilayers similar to cell membranes and can range in size from 20 nm to tens of  $\mu\text{m}$ s. Traditionally, they are formed in bulk-scale systems by several different techniques, including lipid film hydration, reverse phase evaporation, detergent depletion, and alcohol injection.<sup>1</sup> Additional post-formation processing steps, such as sonication or extrusion through a porous track-etch membrane, are often used to obtain smaller and more uniform size distributions.<sup>1</sup> The alcohol injection method has traditionally been performed by injecting lipids dissolved in alcohol into an aqueous buffer solution under strong mixing conditions. To control the mixing conditions better, the alcohol injection method was recently adapted for use in a microfluidic device.<sup>2-5</sup> In this method, the lipid-containing alcohol stream is hydrodynamically focused into a narrow stream by oblique aqueous buffer streams on each side, as shown in Fig. 1. By controlling the flow rates of the alcohol-lipid stream and aqueous buffer streams, the size distributions can be controlled and very narrow size

distributions can be obtained.<sup>2-5</sup> Recently, this method of obtaining controlled mixing was adapted to generate diblock copolymer micelles encapsulating drug nanoparticles.<sup>6</sup> These microfluidic hydrodynamic focusing (MHF) methods could allow drug-liposome formulations to be prepared at the point-of-care, thereby minimizing problems with liposome and/or drug instability over time. In addition, the well-controlled mixing conditions allow the liposome formation process to be studied in more detail. Although theories have been developed for liposome formation in other preparation methods such as detergent depletion and sonication,<sup>7-9</sup> liposome formation is still not well-understood for the alcohol injection method, in which the alcohol-lipid and aqueous solutions are mixed on a time-scale of several ms or less.

The liposomes are hypothesized to form in the microfluidic device because the alcohol and aqueous buffer mix, increasing the polarity of the lipids' solvent, which causes the lipids to become progressively less soluble and to self-assemble into planar lipid bilayers. As these planar bilayer discs grow, they begin to bend to reduce the surface area of hydrophobic chains exposed to polar solvent around the perimeter of the disc. Eventually, these discs close into spherical vesicles with the bilayer separating an aqueous interior from an aqueous exterior, as shown in Fig. 2. The self-assembly process of liposomes using *miscible* solvents differs significantly from other microfluidic microdroplet or microbubble formation methods such as water-in-oil emulsions, double emulsions, or air bubbles.<sup>10-13</sup> Unlike liposomes, microdroplets are formed as a result of mixing immiscible solvents, and the droplets are generally much larger than liposomes. The effect of temperature on the size of microdroplets and microbubbles formed in microfluidic devices was recently studied, and it was found that the droplets and bubbles increased in size with increasing temperature when the solvents were chosen so that the viscosity has a much greater dependence on the temperature than the interfacial surface tension.<sup>13</sup>

Microfluidics provides a convenient means to control both the temperature and the diffusion processes during liposome formation. In this work, we theoretically and experimentally examine how

the liposome size distribution is affected by temperature, phospholipid acyl (hydrophobic) chain length, and flow-rate ratio (FRR) of buffer to alcohol/lipid when using the microfluidic hydrodynamic focusing (MHF) preparation method. Liposomes have a phase transition temperature ( $T_c$ ) below which the bilayer is in a more structured and rigid ripple gel ( $P'_\beta$ ) phase and above which the bilayer is in a more fluid liquid crystalline ( $L_\alpha$ ) phase.<sup>14</sup> The transition temperature increases with acyl chain length for saturated phospholipids. For liposomes formed from pure phosphatidylcholine (PC, see Fig. 2(a)), the transition temperature is -1 °C, 23 °C, 41 °C, and 55 °C for carbon chain lengths of 12, 14, 16, and 18, respectively. Adding cholesterol to the membrane tends to broaden the phase transition measured by differential scanning calorimetry and temperature scanning x-ray diffraction, so that the phase transition occurs through a range of temperatures around  $T_c$ .<sup>15, 16</sup> Because the membrane elasticity modulus is much larger (i.e., the membrane is much stiffer) at or below  $T_c$  compared to above  $T_c$ ,<sup>17</sup> the temperature at which the liposomes are formed relative to  $T_c$  is expected to affect the liposome size, as explained below in the theory section. Published data for the temperature dependence of the elasticity for membranes containing a high percentage of cholesterol (such as the 5:4 phospholipid:cholesterol ratio in this work) is minimal. However, it has been shown that adding cholesterol tends to raise the elasticity modulus<sup>18, 19</sup> and to make the elasticity modulus depend on temperature even at temperatures at least 10 °C to 15 °C above the transition temperature.<sup>20</sup>

The effects of FRR and total volumetric flow rate on liposome size distributions have previously been examined at room temperature for the phospholipid DMPC, which has a transition temperature close to room temperature (23 °C).<sup>2-5</sup> In addition, a different adaptation of the alcohol injection method was recently developed using a very small needle to inject the alcohol/lipid solution into a flowing stream, and it was found that liposomes could only be formed when the solution was heated to above the lipid phase transition temperature, but intermediate temperatures were not examined.<sup>21</sup> Therefore, in this work, we first explore the effects temperature is theoretically expected to have on liposome size

based on a non-equilibrium bilayer planar fragment model. In this model, liposome size is dependent on two rates: the kinetic growth rate of bilayer planar discs and the rate of closure of these discs into spherical vesicles called liposomes. It is shown that for the liposomes in this work, the radius should be approximately proportional to the ratio of membrane elasticity modulus to the line tension of the edges of the bilayer discs. After describing the effects of temperature expected from theory, we form liposomes from four different PC lipids at several temperatures below and/or above the transition temperature and at several flow rate ratios and compare the experimental results to the theoretical expectations.

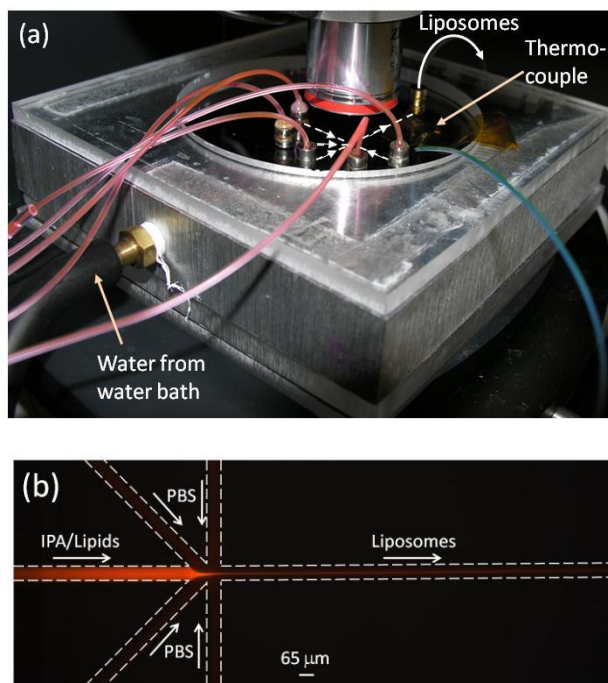


Fig. 1: (a) Photograph of the temperature-controlled aluminum block, on which the microfluidic device and magnetic connectors are placed. Dotted lines and arrows indicate the directions of fluid flow inside the microfluidic device. A thermocouple is taped to the top of the device to measure the temperature. (b) Fluorescent image of the microfluidic hydrodynamic focusing device for liposome formation as seen through the microscope objective shown in (a), in which the isopropyl alcohol (IPA)/lipid mixture containing a fluorescent dye is focused into a narrow stream by four surrounding streams of phosphate

buffered saline (PBS). The liposomes form through self-assembly of the lipid molecules (see Fig. 2), because individual lipids become increasingly insoluble as the alcohol and buffer streams diffusively mix. In this image, the volumetric flow-rate ratio of PBS to IPA/lipids is 29:1.

## Theory

Several models for liposome formation have been proposed, broadly categorized into thermodynamic equilibrium models<sup>8</sup> and kinetic non-equilibrium models.<sup>9</sup> In general, spontaneous equilibrium models are appropriate only for very soft membranes (*i.e.*, the elastic bending energy  $E_b < 0.5 kT$  to  $3 kT$ ), whereas more typical phospholipid membranes (with  $E_b > 10 kT$  to  $100 kT$ ) require kinetic models.<sup>8</sup> Therefore, we use a recently proposed non-equilibrium kinetic model of the liposome formation process for the detergent dilution preparation method.<sup>9</sup> This model is graphically represented in Fig. 2(b). The model proposes that liposome size is determined by two parameters: the growth rate of planar bilayer discs (caused by aggregation of discs) and the rate that the discs close into spherical vesicles (related to a decrease in the bending energy as their sizes and radius of curvature increase). This model was derived and experimentally verified for the detergent dilution liposome preparation method, in which a mixture of concentrated lipid/bile salt micelles is diluted, causing the micelles to fuse into planar lipid bilayer discs, which continue to grow until they close into spherical liposomes.

For alcohol injection liposome preparation methods like our microfluidic hydrodynamic focusing method, it is more difficult to verify the liposome formation process because alcohol-water mixing and liposome formation occur very quickly. Although our system does not include any detergent to stabilize the hydrophobic edges of the planar discs, we hypothesize that the alcohol may stabilize the discs in a similar manner. One difference between our system and the detergent dilution method is that for the detergent dilution method, it is assumed that the discs grow only by aggregation with each other, since individual lipids are very insoluble in water. In contrast, in our system, it may be possible for the discs to

grow both by aggregation with each other and with lipids solubilized in the alcohol/water mixture. However, it is expected that the kinetics of disc growth should depend on temperature in a similar way regardless of the mechanism of growth.

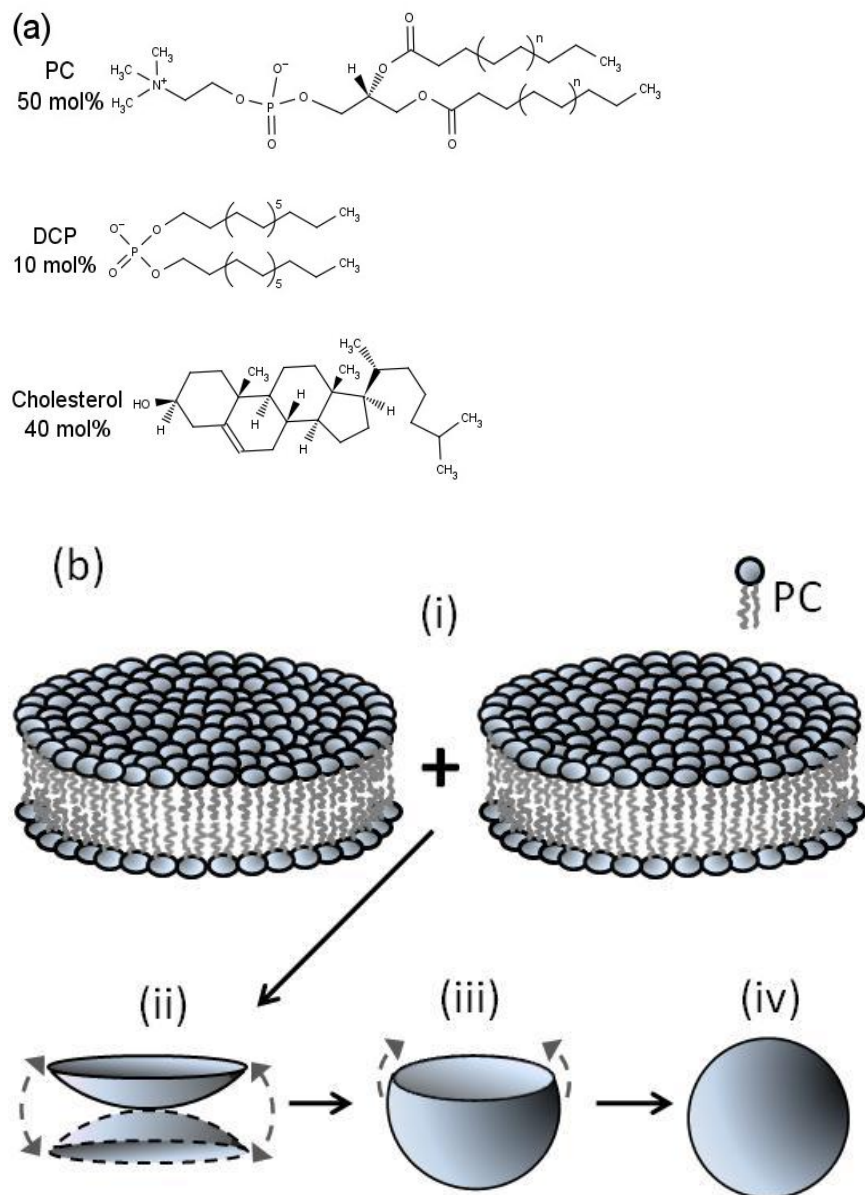


Fig. 2: (a) Structure of components of the liposome bilayer with their mol%. PC represents the phosphocholine lipids used in this work, where  $n = 3, 4, 5,$  and  $6$  for DLPC, DMPC, DPPC, and DSPC,

respectively. DCP (dicetyl phosphate) gives liposomes a negative charge to minimize liposome aggregation. Cholesterol helps stabilize the bilayer. (b) Shows the hypothesized liposome formation mechanism, starting with the aggregation of bilayer planar discs (i), where the hydrophobic chains around the edges are stabilized by alcohol molecules (not shown). These discs grow by combining with each other or individual PC molecules until they are large enough and the alcohol is sufficiently depleted so that they begin to bend (ii) and eventually rapidly close (iii) into spherical bilayer vesicles called liposomes (iv). For graphical clarity, bilayers are depicted with only PC, but membranes in this work include a molar ratio of 5:4:1 of PC:Cholesterol:DCP.

The rate coefficient for the coalescence of lipid bilayer discs ( $K_{ij}$ ) can be expressed from the Smoluchowski equation as:<sup>9</sup>

$$\mathbf{K}_{ij}(T) = \left( \frac{\mathbf{D}_i(T) + \mathbf{D}_j(T)}{\xi^2} \right) S_{ij} \xi e^{-E_{ij}/kT} \quad (1)$$

where the term in parentheses is the attempt frequency for coalescence,  $D_i$  and  $D_j$  are the diffusion coefficients of the two aggregating species,  $\xi$  is the distance over which coalescence can happen,  $S_{ij}\xi$  is the reaction volume, and  $E_{ij}$  is the fusion potential. From the Stokes-Einstein relation,  $\mathbf{D}(T) = k_B T / [6\pi\eta(T)r]$ . In all equations in this paper, terms highlighted in bold change with temperature.

The energy required to close the disc into a liposome (i.e., the “energy of curvature”) depends on the difference between the line energy due to the exposed hydrophobic tails around the edge of the disc and the elastic energy needed to bend the disc into a vesicle. The characteristic closure time  $\tau_c$  for the disc to close into a vesicle decreases exponentially as the energy of curvature increases, as described by Eq. 2.<sup>9</sup>

$$\tau_c(T) = \tau_z(T) \exp \left[ \frac{8\pi\tilde{\kappa}(T)}{kT} \left( 1 - \frac{V_f(T)}{2} \right)^2 \right] \quad (2)$$



where  $\tilde{\kappa}$  is the effective bending elasticity modulus of the membrane, and  $\tau_z(T) = 6\pi\eta(T)r^3/k_B T$  is related to the rotational relaxation time of a disc.  $V_f$  is the vesiculation index, which decreases with stabilization of the hydrophobic edges of the disc, and is defined as:  $V_f = V_0 \left[ 1 + \frac{kT}{\alpha_b} \ln(1 - \varphi_r) \right]$ , where  $V_0 = r\Lambda_0/(4\tilde{\kappa})$  is the vesiculation factor without stabilization,  $\Lambda_0$  is the line tension without stabilization, and  $\varphi_r$  is the fraction of the edge of the disc covered by stabilizing molecules.  $\alpha_b = \Lambda_0 L a_b/A$  is the energy gain from stabilization by one molecule (*e.g.*, isopropyl alcohol in our system), where  $L$  is the circumference of the rim of the bilayer disc,  $A$  is the surface area of the rim, and  $a_b$  is the area covered by one stabilizing molecule. Although the prefactor  $\tau_z$  increases with  $r^3$ , the exponential factor decreases with increasing  $r$  (due to increasing  $V_f$ ), so that the closure time decreases exponentially with increasing radius.<sup>9</sup>

#### *Effect of volumetric flow-rate ratio on liposome size*

For high buffer:alcohol volumetric flow-rate ratios (FRRs), the mixing rate of alcohol/lipids with buffer is increased in two ways. First, the mismatch in fluid velocities at high FRRs decreases the effective diffusion layer thicknesses between the solvents in the focusing region. In addition, higher FRRs decrease the width of the alcohol stream after it is focused, which also decreases the diffusion distances. Since mixing occurs very quickly at high FRRs, the alcohol concentration decreases rapidly (probably faster than the growth rate), leaving the lipid discs to grow with less stabilization from alcohol around the exposed hydrophobic edges. Because  $V_f$  is larger for less stabilized discs, the closure time decreases, so that smaller liposomes are expected to be formed at high FRRs. Conversely, for lower FRRs, the alcohol is depleted more slowly, so that the bilayer discs have more time to grow while they are stabilized by the higher alcohol concentration, resulting in larger liposomes.

#### *Effect of temperature on liposome size*

The temperature affects the growth rate and closure time in multiple ways: (1) by changing the free energy  $k_B T$  and the diffusion coefficients, (2) by changing the viscosity, and (3) by changing the membrane elasticity at or below the transition temperature and by changing the line tension  $\Lambda_0$ . However, in our system, only the changes in membrane elasticity and line tension are expected to change liposome size significantly in most cases, as discussed below.

(1) In the equation for the closure time, the free energy  $k_B T$  is found in the denominators of both the prefactor and the exponential term, so that increasing temperature should decrease the closure times. For the growth rate, according to the Stokes-Einstein relation, the diffusion coefficients increase proportionally to the temperature, and the exponential term also increases with increasing temperature (for positive  $E_{ij}$ ). Therefore, the rate of growth of the lipid bilayer discs is expected to increase with temperature. These changes affect the liposome size in a counteracting manner, so the temperature is not expected to change the liposome size by a large amount due to free energy changes. The free energy may have some effect due to the differences in the exponential terms in the two equations as well as its influence on the vesiculation factor  $V_f$ , but these effects are expected to be much smaller than the effect of membrane elasticity described below.

(2) The viscosity of solutions are generally dependent on temperature.<sup>13</sup> However, any changes in viscosity are not expected to change the liposome size because increasing viscosity both proportionally decreases the growth rate (due to decreased diffusion coefficients) and proportionally increases closure time.

(3) The temperature is expected to affect the liposome size primarily due to its effect on the ratio of the bending elasticity modulus  $\tilde{\kappa}$  to the line tension  $\Lambda_0$ . The bending elasticity has been shown to be two to five times higher (i.e., much “stiffer”) at or below the transition temperature of the lipids compared to above the transition temperature, as shown in Fig. 3.<sup>17,20</sup> Most published data for the dependence of elasticity on temperature is for membranes with pure phospholipid. For pure DPPC or DSPC, the

elasticity continues to increase as the temperature decreases below the transition temperature. For pure DMPC, the elasticity was extremely high at the transition temperature, but unfortunately the elasticity was not measured below the transition temperature. Above the transition temperature, the elasticity changes only minimally for pure phospholipid and is similar for all the lipids, but it increases rapidly when approaching the transition temperature. In contrast, for 7:3 or 1:1 ratios of DMPC:cholesterol, the elasticity modulus becomes larger with increasing concentrations of cholesterol, and the elasticity modulus is still dependent on temperature even above the transition temperature. For membranes containing cholesterol (like those in this work), the elasticity changes with temperature more gradually, and the liposome sizes are expected to be larger even 10 °C to 15 °C above the transition temperature compared to far above the transition temperature.

Neither the line tension nor the elasticity modulus is known for the exact liposome compositions used in this work, and measurements of both variables change by factors of 2 to 10 depending on the measurement technique used. Line tension estimates vary experimentally from 5 pN to 30 pN (1.2  $kT/nm$  to 7  $kT/nm$ ) and theoretically from 50 pN to 60 pN (12  $kT/nm$  to 15  $kT/nm$ ).<sup>22</sup> The temperature dependence of the line tension has not been measured, but theoretically it is expected to decrease with increasing temperature since the entropy of most materials increases with temperature.<sup>23</sup> As seen in Fig. 3, membrane elasticity modulus measurements can vary by a factor of 3 depending on the measurement technique, and they change significantly depending on the concentration of cholesterol in the membrane.

It can be shown that the liposome radius should be approximately proportional to the ratio  $\tilde{\kappa}/\Lambda_0$  under certain conditions: 1) short closure times (i.e., fast mixing), 2) large elasticity modulus (i.e.,  $\tilde{\kappa} \gg kT$ ), and 3) no stabilizing molecules (i.e., at the highest FRRs where IPA is depleted faster than the growth rate). Because liposome size depends on FRR (demonstrated in<sup>2-5</sup> and in this paper), closure time should be smaller than the mixing time, which even for the lowest FRR = 9:1 used in this paper is

less than  $w^2/(2D) \approx (3.25 \text{ } \mu\text{m})^2/(2*10^{-5} \text{ cm}^2/\text{s}) = 5 \text{ ms}$ . The Zimm time  $\tau_z$  is on the order of 0.1 ms (e.g., for  $r = 30 \text{ nm}$ ), so with  $\tilde{\kappa} = 10 \text{ kT}$ ,  $V_f = 1.7$  from Eq. 2. Note that  $\tau_z$  and  $\tau_c$  only have a minimal effect on  $V_f$ , and as  $\tilde{\kappa}$  increases above  $10 \text{ kT}$ ,  $V_f$  will only increase slightly and never become larger than 2. Therefore, if  $\tilde{\kappa} > 10 \text{ kT}$  then  $V_f \approx 2$ , or:

$$V_f = \frac{r\Lambda_0}{4\tilde{\kappa}} \left[ 1 + \frac{kT}{\alpha_b} \ln(1 - \varphi_r) \right] \approx 2 \quad (3)$$

For bilayer discs with edges stabilized by IPA, the  $kT$  factor in Eq. 3 will also cause the liposome size to change with temperature. If the mixing is faster than the growth rate of the bilayer discs, then the IPA molecules will be depleted so that they will have minimal effect on liposome size. If stabilizing IPA molecules can be neglected, Eq. 3 can be simplified to:

$$V_f \approx V_0 = r\Lambda_0/(4\tilde{\kappa}) \approx 2 \quad (4)$$

Eq. 4 is a simple equation from which the ratio of the line tension to the elasticity modulus can be estimated if the liposome radius is measured. For this work, we assume that the mixing is sufficiently fast at FRR = 49:1 to neglect stabilization by IPA, since this is the fastest mixing achievable in our microfluidic device (mixing time  $< 0.2 \text{ ms}$ ). Furthermore, the effect of stabilization by IPA molecules during slower mixing can be estimated by taking the ratio of the radius for slow mixing to the radius for fast mixing, which, from Eqs. 3 and 4, should be equal to  $\left[ 1 + \frac{kT}{\alpha_b} \ln(1 - \varphi_r) \right]$ .

Effects of the temperature on growth rate and closure rate related to variables apart from  $V_f$  are expected only minimally to impact the resulting liposome size. Since  $V_f$  was calculated to be 1.7 for liposomes with the smallest  $r$  and  $\tilde{\kappa}$  and formed at the smallest FRR, and  $V_f < 2$  in all cases, the approximations used in deriving Eqs. 3 and 4 should cause no greater than a 15% error in calculating  $V_f$ . Therefore, in this work, Eqs. 3 and 4 are used instead of Eqs. 1 and 2, which contain additional terms that are not known for the membranes used in this work. By using Eq. 4, fast microfluidic mixing may provide an alternative technique for measure the ratio of elasticity modulus to line tension.

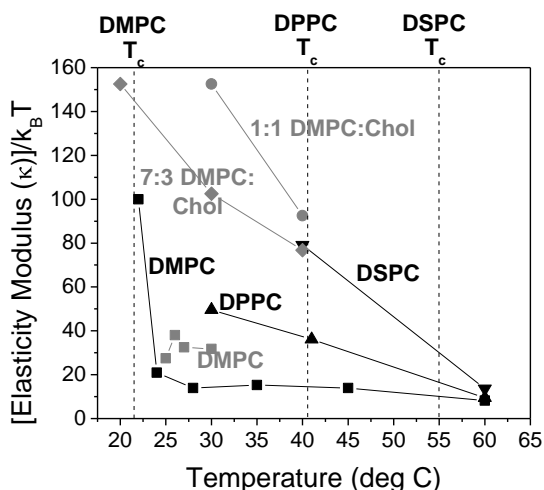


Fig. 3: Bending elasticity modulus of lipid bilayers composed of pure phospholipid or mixtures of phospholipid and cholesterol, from previously published works using neutron spin echo<sup>17</sup> (black points) or thermally excited shape fluctuations of giant unilamellar vesicles<sup>20</sup> (gray points). Vertical dotted lines denote the phase transition temperature ( $T_c$ ) for membranes composed of pure DMPC, DPPC, or DSPC phospholipid. A higher elasticity modulus indicates a more rigid membrane. Elasticity moduli are relatively constant well above  $T_c$  and similar for all pure phospholipid membranes independent of the carbon chain length. Published elasticity temperature dependence data is more limited for membranes containing a high percentage of cholesterol like those in this work, but DMPC membranes containing 30 or 50 mol% cholesterol have elasticity moduli that still depend on temperature 10 °C to 20 °C above the transition temperature.

### Materials/Methods<sup>24</sup>

Phosphate buffered saline packets with pH 7.4 (PBS) were purchased from Sigma Aldrich. Isopropyl alcohol (IPA) was purchased from J.T. Baker, Inc. 1,2-dilauroyl-*sn*-glycero-3-phosphocholine (DLPC, 12:0 PC), 1,2-dimalitoyl-*sn*-glycero-3-phosphocholine (DMPC, 14:0 PC), 1,2-dipalmitoyl-*sn*-glycero-3-phosphocholine (DPPC, 16:0 PC), 1,2-distearoyl-*sn*-glycero-3-phosphocholine (DSPC, 18:0 PC), and

cholesterol were obtained from Avanti Polar Lipids, and dicetyl phosphate (DCP) was obtained from MP Biomedicals. The 100 mm diameter silicon and borosilicate glass wafers were obtained from UniversityWafer.com.

To facilitate flow of fluid through the microfluidic device used to form the liposomes, one end of polypropylene tubing was glued to a magnetic connector with an O-ring between the magnet and the fluidic access port on the microfluidic device, as shown in Fig. 1(a) and as described recently.<sup>25</sup> The opposite terminus of the tubing was pressure fitted into a 0.2  $\mu\text{m}$  filter attached to a syringe. Five of these syringes were placed in syringe pumps (Harvard Apparatus, Model 11 Pico Plus, Holliston, MA) that controlled the flow rates through the five channels shown in the left side of Fig. 1(b). The microfluidic channels were etched in a  $\sim 550 \mu\text{m}$  thick Si wafer using deep reactive ion etching to obtain a width of 65  $\mu\text{m}$  and a depth of  $\sim 260 \mu\text{m}$ . The lengths of the five channels before the intersection were 20 mm and the length of the channel after the intersection was 40 mm. A 500  $\mu\text{m}$  thick borosilicate glass wafer with  $\sim 1$  mm diameter access holes drilled in it was anodically bonded to the Si wafer with the access holes aligned to the ends of the channels. The total volumetric flow rate was 200  $\mu\text{L}/\text{min}$ , with buffer:IPA volumetric flow-rate ratios of 49:1, 29:1, 19:1, and 9:1. The IPA (dehydrated with 4  $\text{\AA}$  molecular sieves, 8 to 12 mesh, from Acros Organics) contained a 5:4:1 molar ratio mixture of PC:Cholesterol:DCP at a total concentration of 5 mmol/L. Buffer and IPA/lipid solutions were degassed by bath sonication at 45  $^{\circ}\text{C}$  to 50  $^{\circ}\text{C}$  before generating the liposomes. The size distributions of the liposomes were obtained using asymmetric flow field-flow fractionation with multi-angle laser light scattering (AFFFF-MALLS using DAWN EOS, Wyatt Technology, Santa Barbara, CA) as described previously.<sup>2-5</sup> Because relatively large liposomes (radius > 50 nm) were obtained in some samples in this work, the Berry plotting formalism was used to fit the angular static light scattering data and calculate the liposome radius.

The temperature of the device was controlled by placing the Si wafer on an aluminum block (see Fig. 1(a)), which had a hole drilled through it parallel to the microfluidic channels so that a water bath (NESLAB RTE-221, Newington, NH) could pump water through the block to regulate the temperature. Thermal contact between the Si wafer and the aluminum block was enhanced by a thin layer of “N grease” (Apiezon Products Ltd., England). Exposed areas of the top and bottom of the aluminum block were covered with ~5 mm-thick sheets of polymethylmethacrylate to reduce convective heat loss. The temperature of the fluids in the device was estimated by taking the average of the temperature of the water bath and the temperature at the top of the glass wafer, measured using a thermocouple and multimeter. The average of these two temperatures was used because this average was approximately the same ( $\pm 1$  °C) as the temperature of the aluminum block measured at any location below the channels without the Si wafer on the block. It is assumed that the thermal conductivity of the Si is sufficient that the temperature of the Si is the same as the aluminum. In addition, the temperatures of the fluids inside the channels are calculated approximately to reach equilibrium before the intersection of fluids at the flow rates used in this work, because ( $\tau_c \approx 1$  ms)  $\ll$  ( $\tau_f \approx 200$  ms), where  $\tau_c$  is the time constant of heat conduction and  $\tau_f$  is minimum amount of time the fluid in the center of the channel takes to travel from the channel entrance to the intersection of the channels.

The statistics package available with Origin was used to compare liposome sizes, by performing one-way analysis of variance (ANOVA) with the Tukey test to compare the individual means.

## **Results/Discussion**

In this study, microfluidic hydrodynamic focusing was used to form liposomes, and the size distributions were determined, with examples shown in Fig. 4. To better understand the formation process, three parameters were varied: phospholipid acyl chain length, buffer-to-alcohol volumetric flow-rate ratio

(FRR), and formation temperature. The dependence of the median liposome radius and size polydispersity on these parameters is shown in Figs. 5 and 6 and discussed below.

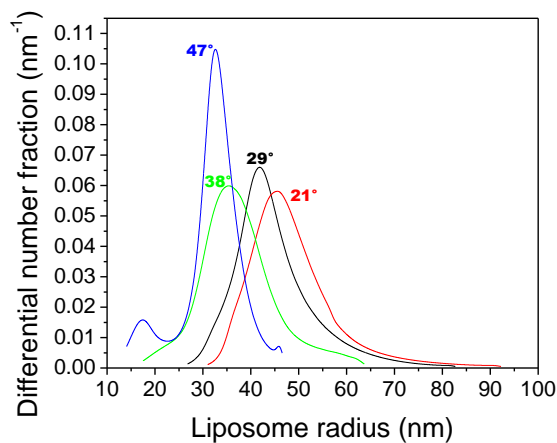


Fig. 4: Example size distributions of 5:4:1 DPPC:Cholesterol:DCP liposomes formed at 47, 38, 29, and 21 °C using microfluidic hydrodynamic focusing with FRR = 29:1. Size distributions were determined using asymmetric flow field flow fractionation combined with multi-angle laser light scattering. The size distributions were normalized so that the area under each curve is equal to one.

#### *Formation below the transition temperature (DPPC and DSPC)*

The long-chain phospholipids DPPC and DSPC have relatively high transition temperatures of 41 °C and 55 °C, respectively. Figs. 5c and 5d show that the liposomes are largest when formed far below the transition temperature and decrease in size as they are formed at temperatures closer to the transition temperature. If it is assumed that the standard deviations for DPPC and DSPC are the same as the corresponding flow rate ratios for DMPC, then the sizes of the liposomes formed at the lowest temperature are significantly ( $p < 0.05$ ) greater than those at the highest temperature for all flow rate ratios except for DSPC at 49:1. The larger liposomes at lower temperatures are most likely due to the much higher elasticity moduli of the membranes below the transition temperature, as discussed above



in the theory section. If the liposomes are formed too far below the transition temperature (e.g.,  $\leq 10$  °C for DPPC or  $\leq 40$  °C for DSPC), then the alcohol stream in the focusing region is not stable and slowly grows over time. Very far below the transition temperature (e.g., at 10 °C for DPPC and 20 °C for DSPC), large visible aggregates begin to form around the alcohol/buffer interfaces in the focusing region. These aggregates at the top and bottom of the channel are likely the cause of the unstable focusing and result in larger and more polydisperse liposomes at lower FRRs, so that very cloudy solution are sometimes obtained at the channel outlet. However, smaller liposomes can be formed at higher flow-rate ratios even at low temperatures, although they are still larger than liposomes formed at the same flow rates at higher temperatures. Therefore, all liposome compositions tested in this paper could be formed into liposomes at or above room temperature for high flow-rate ratios, but liposomes from DSPC may be less reproducible at room temperature due to aggregation and flow fluctuations in the focusing region. The ratio of elasticity modulus to line tension can be estimated from the measurements made with FRR = 49:1. For DPPC, the ratio  $\tilde{\kappa}/\Lambda_0$  clearly decreases from 4.7 nm at 21 °C to 3.6 nm at 47 °C. For DSPC, since the radius does not vary significantly over the temperature range measured in this work, we use the mean radius of 31 nm to calculate  $\tilde{\kappa}/\Lambda_0 \approx 3.9$  nm from Eq. 4. It is unclear why the radius of DSPC liposomes does not depend significantly on temperature for FRR = 49:1, whereas it does depend on temperature for lower FRRs. Further testing would need to be performed to explain this result, since measurements of elasticity modulus and line tension do not exist for the DSPC compositions and temperatures in this work. For DPPC, the effect of alcohol stabilization  $\left(\frac{kT}{\alpha_b} \ln(1 - \varphi_r)\right)$  can be calculated as  $0.09 \pm 0.05$ ,  $0.21 \pm 0.13$ , and  $1.2 \pm 0.4$  for FRR = 29:1, 19:1, and 9:1, respectively. The stabilization effect increases with decreasing FRR as expected since the mixing time increases with decreasing FRR.

*Formation above the transition temperature (DLPC)*

The short-chain phospholipid DLPC has a relatively low transition temperature of  $-1\text{ }^{\circ}\text{C}$ , so it was only possible to form these liposomes above the transition temperature. Fig. 5a shows that the liposome sizes are much less dependent on temperature far above the transition temperature, which is predicted theoretically above because the elasticity modulus is not as dependent on temperature far above the transition temperature. The trends of radius vs. temperature for FRRs of 29:1 and 49:1 are not significant ( $p > 0.05$ ), which is consistent with our theory. For FRRs of 9:1 and 19:1, as the temperature approaches the transition temperature, the sizes generally increase ( $p < 0.01$ ). This trend is most likely because cholesterol and DCP in the membrane cause the membrane elasticity to still be dependent on temperature above the pure DLPC transition temperature. The ratio of elasticity modulus to line tension can be estimated from the measurements made with FRR = 49:1. Since the radius does not vary significantly over the temperature range measured in this work, we use the mean radius of 34 nm to calculate  $\tilde{\kappa}/\Lambda_0 \approx 4.0 \pm 0.7\text{ nm}$  from Eq. 4.

#### *Formation around the transition temperature (DMPC)*

The medium-chain phospholipid DMPC has a transition temperature of  $23\text{ }^{\circ}\text{C}$ , close to room temperature. Interestingly, for volumetric flow-rate ratios at or above 19:1, the largest liposomes are formed around  $29\text{ }^{\circ}\text{C}$ , with significantly smaller liposomes formed at most temperatures above or below  $29\text{ }^{\circ}\text{C}$  (statistical significance is marked by asterisks in Fig. 5b). From the elasticity moduli in Fig. 3 for membranes containing cholesterol, it is not surprising that smaller liposomes are formed at  $37\text{ }^{\circ}\text{C}$ ,  $42\text{ }^{\circ}\text{C}$ , and  $46\text{ }^{\circ}\text{C}$  compared to  $29\text{ }^{\circ}\text{C}$ . However, it is unclear why smaller liposomes are also formed at  $12\text{ }^{\circ}\text{C}$  and  $20\text{ }^{\circ}\text{C}$  compared to  $29\text{ }^{\circ}\text{C}$ . Since membrane elasticity data has not been published for temperatures much below the transition temperature, it is unknown whether the elasticity might be smaller below the transition temperature. In addition, membrane elasticity data has not been published for the membrane composition of 5:4:1 DMPC:Cholesterol:DCP used in this work. It is also possible that the

decreased stability of mixed gel and liquid phase liposomes around the transition temperature may allow for liposome fusion or Ostwald ripening (i.e., free phospholipid molecules inserting into the bilayer) during the formation process at 29 °C, which is not included in our theory. The ratio of elasticity modulus to line tension can be estimated from the measurements made with FRR = 49:1. For example, the liposomes formed at 37 °C had a radius of ~30 nm, so  $\tilde{\kappa}/\Lambda_0 \approx 3.8 \pm 0.4$  nm from Eq. 4. For DMPC, the effect of alcohol stabilization  $\left(\frac{kT}{\alpha_b} \ln(1 - \varphi_r)\right)$  can be calculated as  $0.23 \pm 0.05$ ,  $0.53 \pm 0.14$ , and  $1.3 \pm 0.3$  for FRR = 29:1, 19:1, and 9:1, respectively. Like for DPPC, the stabilization increases with decreasing FRR as expected as the mixing becomes slower. For FRR = 29:1 and 19:1, the stabilization effect is significantly larger than for DPPC ( $p < 0.01$ ), meaning the value of  $\alpha_b = \Lambda_0 L a_0 / A$  is larger for DMPC than DPPC, possibly due to differences in acyl chain lengths since the ratio  $L/A$  will be smaller for DMPC than for DPPC. The line tension  $\Lambda_0$  may also vary with acyl chain length.

### *Polydispersity*

Polydispersity is a measure of the width of the size distribution compared to the median size, where a larger polydispersity indicates a less uniform size distribution. In this work, size fractionation connected to light scattering (AFFFF/MALLS) was used to measure the particle number size distributions, so that the actual size distributions could be measured without any assumptions about the form of the distribution (e.g., the log-normal distribution often assumed with dynamic light scattering). Therefore, polydispersity in this work is defined as  $(R_{75\%} - R_{25\%})/R_{50\%}$ , where  $x\%$  of the total number of liposomes has a size below the radius  $R_{x\%}$ . In Fig. 6, it is clear that the polydispersity increases as the size increases, even though the equation for polydispersity includes the median radius in the denominator. This trend is independent of whether the change in size is due to the formation temperature or the flow-rate ratio, but the polydispersity is smaller for DPPC liposomes than for the other types of liposomes. It is not clear why DPPC liposomes would have a smaller polydispersity than the others since DSPC has a longer acyl

chain length and DLPC and DMPC have shorter acyl chain lengths, but future work could focus on this difference.

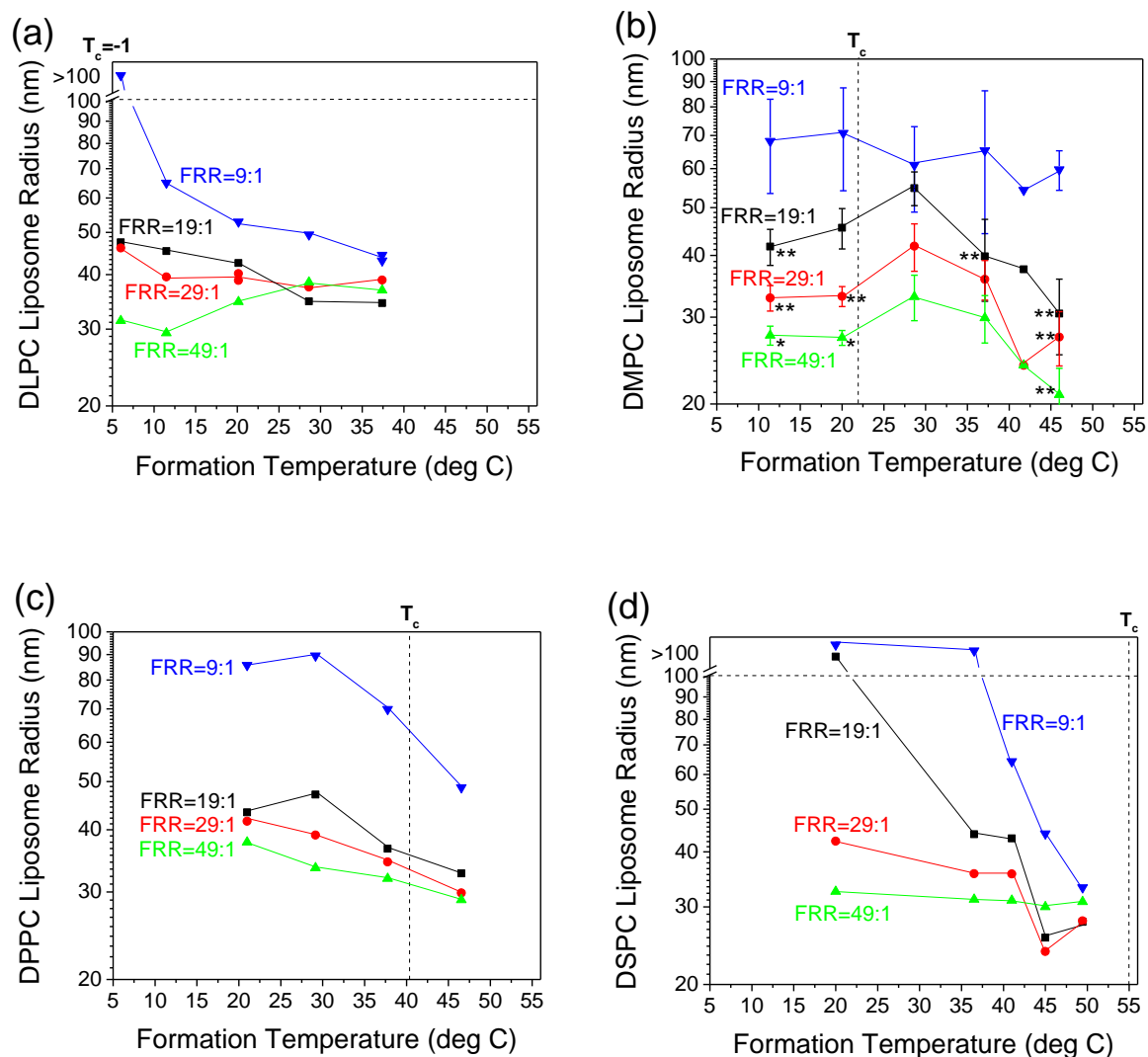


Fig. 5: Median liposome radius vs. formation temperature in the microfluidic device at different volumetric flow-rate ratios (FRRs of 9:1 ( $\blacktriangledown$ ), 19:1 ( $\blacksquare$ ), 29:1 ( $\bullet$ ), and 49:1 ( $\blacktriangle$ )) of buffer to alcohol/lipids for (a) DLPC, (b) DMPC, (c) DPPC, and (d) DSPC. For DMPC, error bars indicate standard deviations ( $n = 2$  to 5) and asterisks indicate that the radius is significantly different from the radius at the same FRR at 27°C (\*\* for  $p < 0.01$  and \* for  $p < 0.05$ ). All other points are from one or two measurements each. The vertical lines indicate the phase transition temperature ( $T_c$ ) for pure phospholipid bilayers (note that the

transition temperature for DLPC is  $-1^{\circ}\text{C}$ ). All radius data is for liposomes containing 5:4:1 molar ratios of PC:Cholesterol:DCP. Note that it was not possible to quantify experimentally median radii above 100 nm using FFF-MALLS, so these data are separated from the others by a horizontal dotted line. These plots demonstrate that liposome size generally increases with the elasticity modulus and does not change significantly far above the transition temperature where the elasticity changes less.

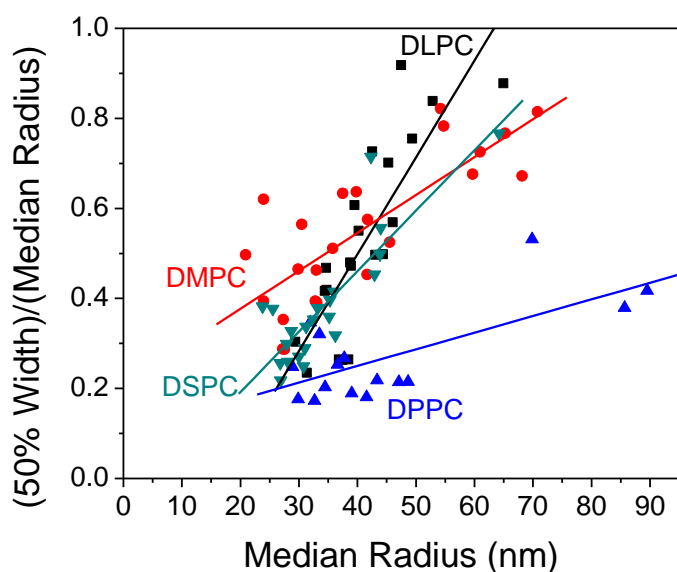


Fig. 6: Size polydispersity vs. median radius for DLPC (■), DMPC (●), DPPC (▲), and DSPC (▼) liposomes formed at all temperatures and flow-rate ratios (i.e., for all data in Fig. 5). The measure of polydispersity used here is the width of the region of the size distribution containing middle 50% of the liposomes, divided by the median radius. The polydispersity generally increases with increasing liposome size, independent of whether the increasing size is due to the formation temperature or the volumetric flow-rate ratio. DPPC liposomes tend to be more uniform in size compared to the other types of liposomes. Lines are fit to points from each liposome composition, with a significant trend ( $p < 0.01$ ) in all cases.

## Conclusions

Temperature has an important influence on the formation of liposomes when produced by microfluidic hydrodynamic focusing of an alcohol/lipid stream. Most liposome formulations qualitatively follow the kinetic theory of liposome formation, in which the liposome size is most influenced by the effect of formation temperature on the line tension and the elasticity modulus of the lipid bilayer at and below the gel-to-liquid crystal phase transition temperature. Due to the “stiffer” membrane below the transition temperature, the planar bilayer discs grow to a larger size before it is energetically favorable to bend and close into a spherical liposome. Although the phase transition is more gradual for the liposomes containing cholesterol used in this work, most compositions still follow this general trend. If the formation temperature is too far below the transition temperature, very large visible lipid aggregates are formed in the focusing region inside the channel at low volumetric flow-rate ratios, often resulting in very cloudy solutions. However, at higher flow-rate ratios it is still possible to form medium-sized liposomes (i.e., radius < 50 nm) below the transition temperature for the liposome compositions used in this work. Liposomes formed from DMPC, cholesterol, and DCP below the transition temperature are an exception to the general rule, but further work measuring the elasticity modulus of these membranes below the transition temperature may help to explain the results. In general, polydispersity depends on the median liposome size, with liposomes becoming more polydisperse as their median size increases, independent of whether the change in size is due to formation temperature or flow-rate ratio. Due to the large difference between the formation processes of liposomes in miscible solvents vs. microbubbles or microdroplets in immiscible solvents, temperature has opposite effects on the liposome and droplet/bubble sizes in these two systems, with the effects of membrane elasticity and line tension dominating during liposome formation and the effect of viscosity dominating during microbubble and microdroplet formation. This work supports the hypothesis that the kinetic liposome formation theory developed previously for detergent dilution liposome formation methods can also be

used to explain liposome sizes obtained in alcohol injection methods such as microfluidic hydrodynamic focusing. In fact, for microfluidic liposome synthesis, the theory can be simplified to show that the liposome radius is approximately proportional the ratio of the elasticity modulus to the line tension of the edges of the bilayer disc. In addition, the theory can be used to approximate the effect of stabilizing molecules (e.g., IPA) on liposome size. Therefore, this theory may be able to be used for the rational design of future microfluidic vesicle synthesis applications. Finally, this work shows that the transition temperature should be taken into account when forming liposomes in microfluidics, especially when forming them far below the lipids' transition temperature.

## Acknowledgments

JMZ acknowledges a postdoctoral fellowship from the National Research Council and helpful discussions with Andreas Jahn. Research performed in part at the NIST Center for Nanoscale Science and Technology. Official contribution of the National Institute of Standards and Technology; not subject to copyright in the United States.

## References

1. G. Gregoriadis, Informa Healthcare, 2007.
2. A. Jahn, W. N. Vreeland, M. Gaitan and L. E. Locascio, *Journal of the American Chemical Society*, 2004, **126**, 2674-2675.
3. A. Jahn, W. N. Vreeland, D. L. DeVoe, L. E. Locascio and M. Gaitan, *Langmuir*, 2007, **23**, 6289-6293.
4. A. Jahn, J. E. Reiner, W. N. Vreeland, D. L. DeVoe, L. E. Locascio and M. Gaitan, *Journal of Nanoparticle Research*, 2008, **10**, 925-934.
5. A. Jahn, S. M. Stavis, J. S. Hong, W. N. Vreeland, D. L. DeVoe and M. Gaitan, 2009, submitted.
6. R. Karnik, F. Gu, P. Basto, C. Cannizzaro, L. Dean, W. Kyei-Manu, R. Langer and O. C. Farokhzad, *Nano Letters*, 2008, **8**, 2906-2912.
7. D. D. Lasic, *Biochemical Journal*, 1988, **256**, 1-11.
8. D. D. Lasic, R. Joannic, B. C. Keller, P. M. Frederik and L. Auvray, *Advances in Colloid and Interface Science*, 2001, **89**, 337-349.
9. J. Leng, S. U. Egelhaaf and M. E. Cates, *Biophysical Journal*, 2003, **85**, 1624-1646.
10. R. C. Hayward, A. S. Utada, N. Dan and D. A. Weitz, *Langmuir*, 2006, **22**, 4457-4461.

11. T. Thorsen, R. W. Roberts, F. H. Arnold and S. R. Quake, *Physical Review Letters*, 2001, **86**, 4163-4166.
12. I. Shestopalov, J. D. Tice and R. F. Ismagilov, *Lab on a Chip*, 2004, **4**, 316-321.
13. C. A. Stan, S. K. Y. Tang and G. M. Whitesides, *Analytical Chemistry*, 2009, **81**, 2399-2402.
14. G. Cevc, *Biochemistry*, 1987, **26**, 6305-6310.
15. S. Imaizumi and I. Hatta, *Journal of the Physical Society of Japan*, 1984, **53**, 4476-4487.
16. I. Hatta, 2005, pp. 189-192.
17. Z. Yi, M. Nagao and D. P. Bossev, *Journal of Physics-Condensed Matter*, 2009, **21**, 155104.
18. A. Hodzic, M. Rappolt, H. Amenitsch, P. Laggner and G. Pabst, *Biophysical Journal*, 2008, **94**, 3935-3944.
19. J. Henriksen, A. C. Rowat, E. Brief, Y. W. Hsueh, J. L. Thewalt, M. J. Zuckermann and J. H. Ipsen, *Biophysical Journal*, 2006, **90**, 1639-1649.
20. P. Meleard, C. Gerbeaud, T. Pott, L. FernandezPuente, I. Bivas, M. D. Mitov, J. Dufourcq and P. Bothorel, *Biophysical Journal*, 1997, **72**, 2616-2629.
21. P. Pradhan, J. Guan, D. Lu, P. G. Wang, L. J. Lee and R. J. Lee, *Anticancer Research*, 2008, **28**, 943-947.
22. S. Baoukina, L. Monticelli, H. J. Risselada, S. J. Marrink and D. P. Tieleman, *Proceedings of the National Academy of Sciences of the United States of America*, 2008, **105**, 10803-10808.
23. M. F. Luo, Y. H. Sua, G. R. Hu, C. H. Nien, Y. W. Hsueh and P. Chen, *Thin Solid Films*, 2009, **517**, 1765-1769.
24. Certain commercial equipment, instruments or materials are identified in this report to specify adequately the experimental procedure. Such identification does not imply recommendation or endorsement by the National Institute of Standards and Technology, nor does it imply that the materials or equipment identified are necessarily the best available for the purpose.
25. J. Atencia, G. A. Cooksey, A. Jahn, J. M. Zook, W. N. Vreeland and L. E. Locascio, *Lab Chip*, 2010, **10**, 246-249.